Vibrational energy funneling in viruses—simulations of impulsive stimulated Raman scattering in M13 bacteriophage

2009 J. Phys.: Condens. Matter 21 505102

(http://iopscience.iop.org/0953-8984/21/50/505102)

J. Phys.: Condens. Matter **21** (2009) 505102 (6pp) doi:10.1088/0953-8984/21/50/505102

Vibrational energy funneling in viruses—simulations of impulsive stimulated Raman scattering in M13 bacteriophage

Eric C Dykeman[1] **and Otto F Sankey**[2]

[1] Department of Biology, University of York, YO10 5DD, UK
[2] Department of Physics, Center for Biological Physics, Arizona State University, Tempe, AZ 85287, USA

Received 2 July 2009, in final form 30 September 2009
Published 13 November 2009
Online at stacks.iop.org/JPhysCM/21/505102

Abstract
The vibrational excitation of a tubular M13 bacteriophage capsid is simulated using classical molecular dynamics. The excitation occurs through impulsive stimulated Raman scattering by ultra-short laser pulses which ping the vibrational modes of the capsid. Tuning the laser pulse temporal width determines the frequency region of the capsid that is excited. The simulations reveal that electromagnetic energy transferred to the high frequency modes by ultra-short pulses is funneled via anharmonicity to just five low frequency modes which receive approximately 80% of the funneled energy. A single mode receives most of the funneled energy (3–4% of the total energy delivered) involves swelling and is effective in damaging the capsid. However, the laser intensity necessary to produce damage to the capsid from a single laser pulse is found to be extremely high for this mechanism to be effective.

(Some figures in this article are in colour only in the electronic version)

1. Introduction

The current paradigm for treatment and prevention of viral infections relies heavily on chemical methods such as vaccination and drugs. Vaccination is the primary tool in the arsenal of preventative viral treatments and acts to engage an immune system response producing antibodies and preventing an acute infection from occurring. If no vaccine is available or if one is rendered useless due to mutations of the virus, an acute infection can occur. Treatment options are limited and usually attempt to suppress further accumulation of virus in the body. One example of such treatment is the drug regimens used to treat HIV infection that target viral specific enzymes, minimizing symptoms and slowing progression of disease.

Since viruses have no metabolism of their own, they must commandeer the metabolism of their host cell in order to replicate. As a result, their life cycle is extremely short and they typically rely on the host cells protein machinery for the necessary enzymes required for replication. This limits options for attacking a virus since chemicals that target the viruses life cycle could potentially target the host cells protein machinery which is critical to keeping the host cell (and other uninfected cells) alive. In the case of HIV treatments, the rapid replication of viral particles allows for high mutation rates that can quickly render a drug treatment ineffective. Thus, new methods of treatment that can avoid these problems are needed.

One method which shows some promise is to attack a virus mechanically by stimulating the vibrational modes of the virus' protective protein capsid. Tsen and colleagues [1, 2] have shown that the M13 bacteriophage virus and other pathogens can be inactivated by short laser pulses, in a mechanism believed to be impulsive stimulated Raman scattering (ISRS) [3]. The ISRS process is mechanical and acts on the virus through its vibrational modes. Thus ISRS treatments are likely to avoid mutation problems. In addition, these first ISRS experiments suggest that the method is selective, i.e. a window in laser pulse width and intensity exists such that viruses and other pathogens can be targeted while leaving healthy cells undamaged [4]. An immediate potential therapy would be the cleansing of blood contaminated with viral/microbial particles.

Despite these very early successes, it remains unclear if ISRS is the sole mechanism (or even the most important mechanism) involved in the inactivation of M13 seen in experiment. To study how ISRS could potentially result in the inactivation of viruses, an initial basic qualitative understanding of how the mechanical modes of a virus are stimulated by ISRS is required. The ISRS simulations reported here are the very first of their kind and seek to begin the process of interpreting the experimental results. This work examines how the pulse width of the incident light effects the time evolution of the kinetic energy in the lowest 145 harmonic modes of the M13 bacteriophage using classical molecular dynamics (MD) simulations.

Our main conclusions is that short laser pulses directly excite high frequency modes of the capsid but anharmonic processes quickly dump a significant fraction of that energy into low frequency global cooperative modes of the virus capsid. Additionally, as found earlier [5], the incident photon energy flux of a single pulse needed to produce damage by the impulsive stimulated Raman scattering (ISRS) mechanism is extremely high.

We organize the paper as follows. First we give a brief description of the ISRS light scattering process where light interacts with a viral particle through its electronic polarization response. Using a bond polarizability model for the polarization field of the virus, we derive a simple formula for the time dependent ISRS force on a single covalent bond which can be easily implemented in an MD protocol. Next we perform a series of MD simulations on the M13 bacteriophage which incorporate an additional force on the bonds in the protein capsid resulting from ISRS. Using the displacement patterns of the 145 lowest frequency modes (determined to atomic resolution in earlier work [6]) we monitor the time evolution of the kinetic energy in the 145 lowest normal modes. Finally we conclude the work and point out the inconsistencies between theory and experimental studies of light scattering from viral particles.

2. Theoretical background

The absorption effects of electric fields on proteins have been explored in the past using MD. For example, English and Mooney have studied the denaturation of hen egg white lysozyme using a continuous wave electric field which interacts with the protein via the Lorentz force [7]. In this case, the light interacts with the protein by creating a harmonic driving force on the atoms at the frequency of the incident light. Since the *low* frequency vibrational motions of proteins and viruses are expected to be on the order of a few cm^{-1} the frequency of light must be in the gigahertz (microwave) to terahertz (T-wave) range in order to produce an oscillation. These frequencies do not penetrate water well. An alternate mechanism is ISRS which can be used with visible light. ISRS is a scattering process in which only bound electrons follow the rapid oscillations of light, while the forces on the nuclei are proportional to the modulation envelope of the light intensity (e.g. equation (3) below). For an ultra-short laser pulse, ISRS leads to an impulsive force on the protein's atoms that follow the pulse shape of the light, assumed here to be a Gaussian with pulse width τ_L (of order 1 ps). Thus, ISRS allows the wavelength of light to be in the near-IR to visible spectrum since the pulse width determines the region of the virus' vibrational spectrum that will be excited (see equation (7) and accompanying text).

We model the ISRS process in a simple, yet effective manner, so that the resulting description can be incorporated into an MD protocol. Raman scattering is produced by the induced electronic polarization, which has a complex dependence on the electronic structure of the molecule. At the present time, the polarization field of a virus is extremely difficult to compute using a first principle approach. Thus, we use a simplified bond polarizability (BP) model to describe the polarization field of the virus. The BP model has been quite successful at predicting Raman scattering profiles of small molecules such as C_{60}, C_{70}, and hydrocarbons using a set of fitted parameters [8–10]. Tsen and colleagues [11] have measured the low frequency Raman spectra profile of M13 phage and found a single broad peak at roughly 8.5 cm^{-1} with an intensity that is proportional to viral concentration. Our recent work [6] has shown that, using an atomic description of the vibrational mode patterns, the BP model is capable of reproducing the single broad peak seen in the experimental Raman scattering profiles of the M13 bacteriophage virus using only a single set of BP parameters. This suggests that (i) the BP model is a reasonable starting point for studying the ISRS process (ii) the frequency spectrum of our low frequency modes are in relatively good agreement with experiment.

In the BP model, each individual covalent[3] bond b between atoms i and j in the protein structure of the virus has a polarizability tensor $\overleftrightarrow{\alpha}_b$ given by

$$\overleftrightarrow{\alpha}_b = \alpha_\parallel \hat{P} + \alpha_\perp (\hat{I} - \hat{P}). \tag{1}$$

The operator $\hat{P}$ is the bond projection operator, $\hat{P} = |\hat{d}\rangle\langle\hat{d}|$, where $\hat{d}$ is the normalized bond direction obtained from $\vec{d} = \vec{r}_i - \vec{r}_j$. The total polarizability of the entire virus is then simply the sum over all bonds in the protein network, $\overleftrightarrow{\alpha} = \sum_b \overleftrightarrow{\alpha}_b$. This assumes that the laser frequency is low enough that there are no electron resonance or transition effects.

The electric field of the pulsed laser is assumed to take the form $\vec{E}(t) = \vec{E}_0 e^{-t^2/2\tau_L^2} \cos(\omega_L t)$, where the peak electric field amplitude has been chosen to occur at $t = 0$. The spatial dependence of the electric field has been neglected due to the relatively long wave length of the light used in ISRS experiments (~600–800 nm) when compared with the dimensions of a single bond or protein. The ISRS electric field induces [3] a time dependent polarization field $\vec{P}(t)$ on the virus, $\vec{P}(t) = \overleftrightarrow{\alpha}\ \vec{E}(t)$. The energy required to build up the polarization field of the virus is

$$U(t) = -\tfrac{1}{4}\vec{E}_0 \cdot \overleftrightarrow{\alpha} \cdot \vec{E}_0 e^{-t^2/\tau_L^2}, \tag{2}$$

where the oscillatory dependence has been time averaged due to the short period of visible light (2 fs for 600 nm light). The

[3] Weaker hydrogen and van der Waals 'bonds' are not considered to contribute significant polarization effects.

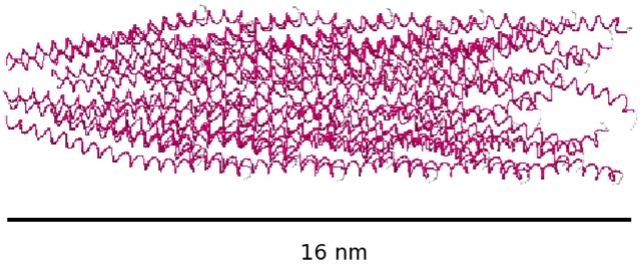

Figure 1. Periodic segment of the M13 bacteriophage protein capsid. The total length of the segment is 161.5 Å with the tube axis along $\hat{z}$.

time dependent force on each atom i in the virus due to light scattering is then obtained via $F^{\mathrm{L}}_{i\beta}(t) = -\partial U(t)/\partial r_{i\beta}$ where $\beta = x, y, z$. Assuming small bond oscillations, the result for a single covalent bond containing atom i is

$$F^{\mathrm{L}}_{i\beta}(t) = [f_d \hat{d}_\beta + f_E \hat{E}_{0\beta}] \frac{|E_0|^2}{4} \mathrm{e}^{-t^2/\tau_{\mathrm{L}}^2}, \tag{3}$$

where the functions f_d and f_E are given by

$$\begin{aligned} f_d &= (\hat{E}_0 \cdot \hat{d})^2 \left[\alpha'_\parallel - \alpha'_\perp - \frac{2(\alpha_\parallel - \alpha_\perp)}{d}\right] + \alpha'_\perp, \\ f_E &= (\hat{E}_0 \cdot \hat{d}) \frac{2(\alpha_\parallel - \alpha_\perp)}{d}. \end{aligned} \tag{4}$$

Given the electric field orientation $\hat{E}_0$, pulse width of the light τ_{L}, light intensity $I \propto |E_0|^2$, and three polarizability parameters of the bond ($\alpha'_\parallel$, $\alpha'_\perp$, and $(\alpha_\parallel - \alpha_\perp)/d$), equations (3) and (4) determine the additional force from ISRS for use in an MD protocol.

3. Computational methods

The ISRS MD simulations were performed on the M13 bacteriophage, a tubular virus of roughly 800 nm in total length. The simulations employ periodic boundary conditions (PBC) on a small segment of the virus (figure 1), which mimic the quasi-momentum conservation observed in Raman scattering where the excited wavevector satisfies $k \approx 0$. The segment is built from 50 alpha helical protein building blocks (PDB ID = 2C0W) which consist of 50 amino acids each [12]. The resulting unit cell contains $N = 37\,050$ atoms with the tube axis along the z direction. The lattice vector in the z direction was set to 161.5 Å while the remaining lattice vectors (along x and y) are set to 250 Å to avoid Coulombic interactions with cells perpendicular to the tube axis. Since we seek an initial qualitative understanding of ISRS, interactions of the protein capsid with the viruses circular ss-DNA and explicit water molecules are neglected. The energetic effects of water are incorporated using the implicit solvent generalized Born model [13–15], which uses a dielectric screening methodology allowing the Coulomb sum to be truncated and avoiding the traditional Ewald sum. A cutoff of 10 Å was used for all calculations reported here.

The neglect of interactions of the capsid with the virus' genome and explicit water could have consequences for the simulation. In some viruses (e.g. MS2 phage) coat protein–ss-RNA interactions appear to affect the assembly pathway of the viral capsid [16]. In this virus (and other ss-RNA viruses) it is clear that electrostatic interactions of the genome with the capsid protein are quite strong and are crucial for efficient assembly of the viral particle. For other viruses, particularly M13 in this case, the strength of the electrostatic interactions between nucleic acid and coat proteins is not as clear. For M13 phage, the genome of the virus is transported to the cell membrane by a DNA binding protein (p5) where it is replaced by the capsid protein (p8) which is in complex with the cell membrane [17]. Thus although the capsid protein has some interaction with genomic material, it is likely weak. Likewise, the inclusion of explicit water is important for understanding the role of solvent damping on the ISRS process. The experimental measurement of the Raman spectra profile of M13 in water [11] and the agreement with the theoretical Raman spectra profile [6] provides some evidence that the mechanical modes are not overdamped.

Starting from a minimized structure of the M13 capsid with an initial kinetic energy of zero ($T = 0$ K), a series of constant energy constant volume MD simulations using the empirical AMBER energy model [18] with the additional force from a ISRS light pulse (equations (3) and (4)) were performed at various pulse widths of light τ_{L}. Here constant energy means that energy does not flow to or from a surrounding heat bath although energy can still be gained or lost from the interaction with light. While temperature and solvent dampening effects are likely to play key roles, removing these effects allows a clear qualitative picture of which vibrational modes gain or transfer kinetic energy from the light pulse to emerge.

Each covalent bond in the protein network is given the same three BP parameters of $\alpha'_\parallel = 2.89$ Å^2, $\alpha'_\perp = 0.33$ Å^2, and $(\alpha_\parallel - \alpha_\perp)/d = 1.04$ Å^3, which correspond to those of hydrocarbons [10]. The light intensity and electric field direction were set to $I = 0.1 - 2$ PW cm^{-2} and $\hat{E}_0 = \hat{z}$. In classical MD, it is found that the ISRS force is extremely weak and large intensities of at least 10^4 higher than experiment are used to amplify the disturbance produced by a *single* pulse [5], while experiments [1, 2, 4] produce $\sim 10^6$ pulses s^{-1} ($\sim$MHz rates). Thus, damage to the capsid can be severe from a single pulse in the simulation while experimentally the damage is (presumably) small per pulse, but accumulative. Even with the large laser intensities, additional atomic forces are of order 1 eV Å^{-1}.

The 145 low frequency normal modes used for the analysis were obtained using harmonic analysis from earlier work [6] which employed the same potential energy model used in the MD simulations. The frequency of the modes range from 1.45 to 8.77 cm^{-1} and the displacement patterns $|\eta_\nu\rangle$ of mode ν were determined with atomic detail using the phonon functional method [19]. The vectors $|\eta_\nu\rangle$ are determined from the orthonormal eigenvectors $|e_\nu\rangle$ of the dynamical matrix through $|\eta_\nu\rangle = \overleftrightarrow{M}^{-1/2} |e_\nu\rangle$, where $\overleftrightarrow{M}$ is the diagonal mass tensor. Although the vibrational modes are only valid at the local minimum where they were calculated, they form a complete orthonormal basis (or equivalently a set of principal

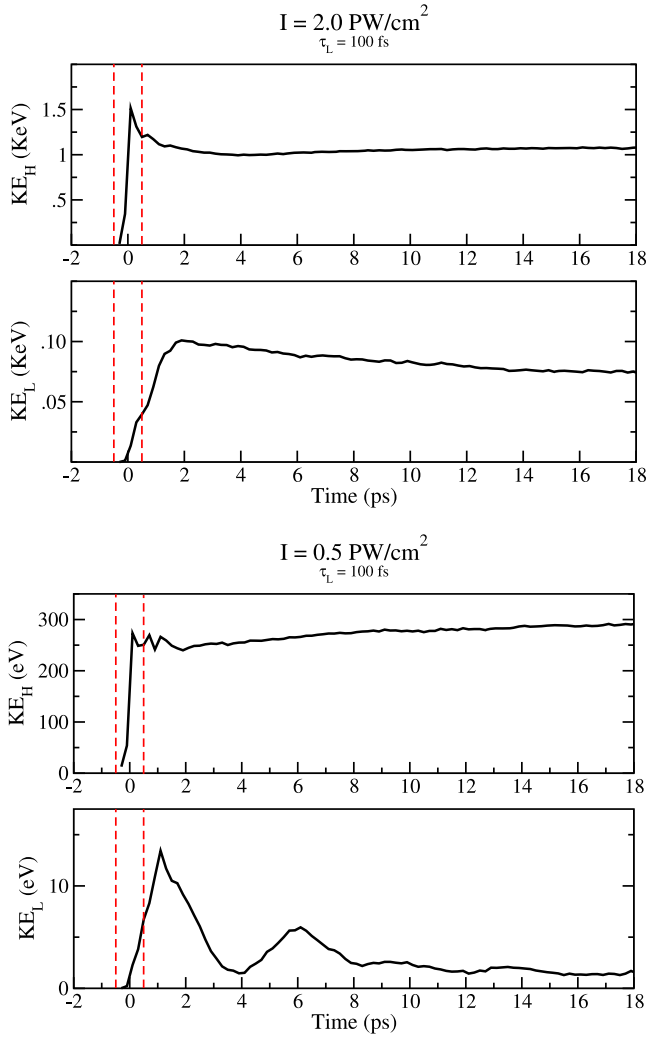

Figure 2. Kinetic energy in the high frequency modes (upper panels) and low frequency modes (lower panels) of ISRS stimulated M13 bacteriophage as a function of time for two peak light intensities: (a) $I = 2.0$ PW cm^{-2}; (b) $I = 0.5$ PW cm^{-2}. A thermal kinetic energy of $\frac{3}{2}kT$ for 37 050 atoms at room temperature corresponds to 1.4 keV. The pulse width of the incident light was $\tau_L = 100$ fs. The dashed red lines indicate roughly the times $t = \pm 5\tau_L$ when the capsid interacts with the light.

components) that can be used to extract information on the amount of kinetic energy in each mode. We combine normal mode analysis with MD to determine the kinetic energy of each mode $|\eta_\nu\rangle$ from the MD velocity vector $|v(t)\rangle$ (of length $3N$ with $N = 37\,050$) as a function of time. The velocity vector can be expanded in terms of the displacement vectors (complete set) from the normal mode analysis,

$$|v(t)\rangle = \sum_{\nu=1}^{3N} \dot{Q}_\nu(t)|\eta_\nu\rangle. \tag{5}$$

The kinetic energy in mode ν is simply $\mathrm{KE}_\nu(t) = \dot{Q}_\nu^2(t)/2$. To obtain $\dot{Q}_\nu(t)$ from the MD simulation we project the velocity vector onto the mode displacement using the mass matrix,

$$\mathrm{KE}_\nu(t) = \tfrac{1}{2}|\langle\eta_\nu|\overleftrightarrow{M}|v(t)\rangle|^2. \tag{6}$$

For a system driven by ISRS that is perfectly harmonic [3], $Q_\nu(t) \propto \cos(\omega_\nu t)$ and the amplitude $Q_{0,\nu}$ of the mode at long times (neglecting dampening) is proportional to

$$Q_{0,\nu} \propto (\tau_L/\omega_\nu)\, \mathrm{e}^{-\omega_\nu^2\tau_L^2/4} \tag{7}$$

while the energy is proportional to

$$E_\nu = [\mathrm{KE}_\nu]_{\max} \propto \tau_L^2\, \mathrm{e}^{-\omega_\nu^2\tau_L^2/2}. \tag{8}$$

The amplitude of the mode is a Gaussian function of the modes frequency ω_ν which results in the ISRS effect coupling strongest ($\mathrm{d}Q_{0,\nu}/\mathrm{d}\tau_L = 0$) to a pulse time which satisfies $\omega_\nu\tau_L = \sqrt{2}$, or in terms of the period of the normal mode, $\tau_L = 0.225T_\nu \approx T_\nu/4$. Thus high frequency modes are excited by short pulses while low frequency modes are excited by long pulses, consistent with a time × frequency uncertainty relationship. Using a qualitative acoustic model of the density of states in 3D, ($D(\omega) \propto \omega^2$), one can obtain a qualitative formula for the total energy deposited (TED) in the viral capsid from ISRS as TED $\propto I^2/\tau_L$. This counter-intuitive result indicates that short pulses deposit more energy into the capsid than long pulses. The reason for this is that low frequency modes are sparse (low $D(\omega)$) while high frequency modes are dense.

4. Results and analysis

We break the frequency spectrum into two regions—low frequency (less than 8.77 cm^{-1}) and high frequency (greater than 8.77 cm^{-1}). The low frequency modes simply correspond to the 145 normal modes we have computed, and high frequency are the $3N - 145$ (=111 005) remaining modes. Figure 2 illustrates the kinetic energy in the high frequency modes (upper panels) and in the low frequency modes (lower panels) as a function of time. The laser pulse time is $\tau_L = 100$ fs which most effectively stimulates modes near 75 cm^{-1} ($\omega_\nu\tau_L = \sqrt{2}$). Two intensities of light are shown, $I = 2.0$ PW cm^{-2} in figure 2(a), and $I = 0.5$ PW cm^{-2} in figure 2(b). The dashed lines indicate the times of $t = \pm 5\tau_L$, extreme limits when the light pulse intensity can be considered 'on' ($I = I_0\mathrm{e}^{-t^2/\tau_L^2}$). For either intensity, the maximum kinetic energy given to the high frequency spectrum occurs near $t = 0$ when the light intensity is also maximum. The low frequency modes ($\omega \leqslant 8.77$ cm^{-1}) however have almost no kinetic energy at $t = 0$. Instead, they gradually buildup their kinetic energy reaching a maximum at ∼1.5–2.0 ps, well after the light pulse is gone. This delay suggests that anharmonicity transfers energy from modes near 75 cm^{-1} to the low frequency modes. An analysis of the amount of kinetic energy transferred reveals that 5 modes receive ∼80% of the transferred energy with the radial breathing (swelling) mode at 5.22 cm^{-1} receiving over 50% of it, which is about 3.5% of the *total* kinetic energy delivered to the capsid. Table 1 summarizes the data for the $I = 2.0$ PW cm^{-2} simulation. Simulations at lower intensities (table 2) show that this anharmonic funneling effect persists. These data show that there exists an effective funneling mechanism that drives energy from modes 15 times

Table 1. Maximum kinetic energy gained by 5 low frequency modes from anharmonic coupling. The intensity of light was 2.0 PW cm^{-2} with a pulse width of 100 fs. KE_L is the percentage of kinetic energy in the mode normalized to the lowest 145 modes while KE_T is normalized to the total in all modes. The * indicates the swelling mode.

ω	KE_L (%)	KE_T (%)
4.98	5.30	0.35
5.01	2.34	0.15
5.13	8.47	0.56
5.19	12.30	0.81
5.22*	52.86	3.46
Total	81.27	5.33

Table 2. Maximum kinetic energy gained in the lowest 145 modes (KE_L) and the remaining high frequency modes (KE_H) of the M13 capsid for various intensities of light. The pulse width is 100 fs. Intensities are in PW cm^{-2} and energies are in eV. The per cent transferred via funneling is the ratio of KE_L to KE_H times 100.

I	KE_L	KE_H	Transferred (%)
0.1	2.88	57.391	5.02
0.5	10.26	273.20	3.75
1.0	17.86	641.97	2.78
1.5	53.66	1085.4	4.94
2.0	99.12	1513.1	6.55

higher in frequency to the low frequency swelling and a handful of other global modes.

It is quite remarkable that 3.5% of the kinetic energy delivered by the laser is contained in just one of 111 150 modes when that mode is not directly excited by the laser very much. To get an idea of how severe this is, the energy peak for the low frequency modes in the higher intensity simulation (figure 2(a), lower panel) has quantum number $n \sim 150\,000$ ($E = \hbar\omega(n + 1/2)$). The high intensity simulation was sufficient to separate the individual protein building blocks into monomers through a radial expansion consistent with the swelling mode. The lower intensity simulation (figure 2(b)) produced large amplitude oscillations but recovered. For the lower intensity, the kinetic energy in the low frequency modes roughly follow that of a damped harmonic oscillator with period ∼4–7 ps, which is consistent with the period (6.4 ps) of the 5.22 cm^{-1} swelling mode.

To further understand this funneling phenomenon and its dependence on pulse width, ISRS MD simulations were performed at pulse widths ranging from $\tau_L = 2$ ps to 2 fs. For each simulation, the maximum kinetic energy in the swelling mode at 5.22 cm^{-1}, was determined. Figure 3 shows the results and illustrates the concept of 'direct' and 'coupled' ISRS effects. The direct ISRS effect refers to excitation of the mode by forces directly from the laser light. The maximum direct ISRS excitation of a mode of frequency ω_ν occurs when $\tau_L = \sqrt{2}/\omega_\nu$. The 5.22 cm^{-1} swelling mode will be strongly excited by the direct ISRS effect when the pulse time of light is near 1500 fs (1.5 ps). The abscissa of figure 3 is the pulse time while the upper scale indicates the vibrational frequency $\omega_\nu = \sqrt{2}/\tau_L$ where that frequency gains the strongest boost. Figure 3 makes clear that the energy delivered to the 5.22 cm^{-1}

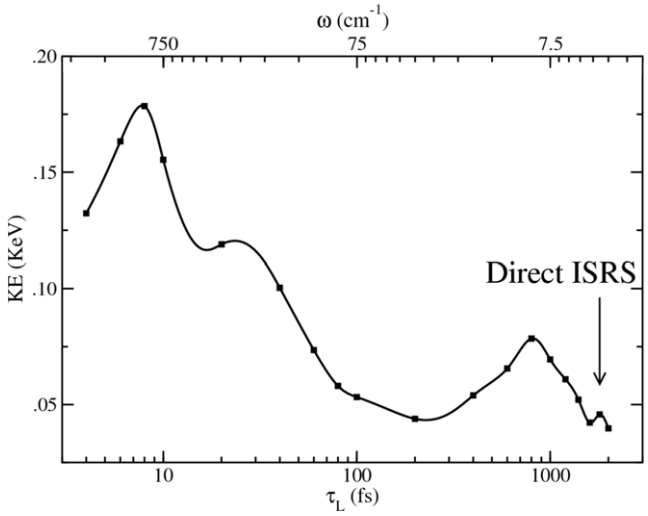

Figure 3. Maximum kinetic energy delivered to the 5.22 cm^{-1} radial breathing (swelling) mode of ISRS stimulated M13 bacteriophage as a function of laser pulse time τ_L. A mode of frequency ω is excited most when the pulse time τ_L satisfies $\omega_\nu \tau_L = \sqrt{2}$. The frequency ω that satisfies this is indicated on the upper scale. Data points (solid squares) are interpolated with a cubic spline.

swelling mode is fairly small near the direct ISRS coupling, but is excited far more by much *shorter* pulse times which excite higher frequency modes.

The cause of this is clear—the energy delivered to the capsid in ISRS is roughly predicted to scale as I^2/τ_L. Thus shorter pulse widths deliver *more* total energy to the M13 capsid. But this energy is not delivered specifically at the swelling (disassemble) mode at 5.22 cm^{-1}. Anharmonic coupling amongst modes transfers some of this energy to low frequency modes. In fact, due to a remarkable funneling effect, a significant fraction goes into the single 5.22 cm^{-1} swelling mode. The funneling effect of the anharmonic coupling along with the $1/\tau_L$ dependence on the TED creates a situation where very short pulse times can influence the swelling mode more strongly than direct ISRS through this 'coupled' ISRS effect. This provides a possible explanation for the sharp cutoff in M13 inactivation observed in experiment [4] where only short pulse widths (<500 fs) inactivate M13.

5. Conclusion

Although much work remains to be done regarding ISRS MD simulations of viral capsids, notably the addition of solvent dampening effects, the work presented here provides an understanding of the basic physics involved and provides a foundation for future work. A surprising result of this study was the strong anharmonic coupling of vibrational modes to the radial breathing (swelling) mode, suggesting an underlying energy landscape which tends to funnel energy to this mode. This funneling behavior is likely to play a role in other forms of vibrational energy transfer from high frequency excitations to low frequency excitations such as energy transfer after optical absorption, or for 2-phonon absorption processes of low frequency laser light. The high

intensities needed to produce damage in the simulations is in serious disagreement with experiments [1, 2, 4]. Experiments typically use 100 GW cm^{-2} intensities or less to produce damage with pulses that repeatedly strike the virus (pulses are sent at MHz rates). We also note that theoretical calculations of the binding energies of capsid proteins are typically in the 15–150 kcal mol^{-1} range and sometimes higher, which is in disagreement with experimental estimates of the binding energies (3–5 kcal mol^{-1}) [20]. These issues may explain the disagreement between experiment and theory. Other mechanisms, such as two-photon absorption processes, are alternate mechanisms for producing virus damage. Further exploration of these alternate mechanisms are necessary to obtain a complete understanding of the interaction of ultrashort laser pulses with viruses with the aim of inactivating them.

References

[1] Tsen K-T, Tsen S W D, Chang C L, Hung C F, Wu T C and Kiang J G 2007 Inactivation of Viruses by coherent excitations with a low power visible femtosecond laser *Virol. J.* **4** 50

[2] Tsen K-T, Tsen S-W D, Chang C-L, Hung C-F, Wu T-C and Kiang J G 2007 Inactivation of viruses with a very low power visible femtosecond laser *J. Phys.: Condens. Matter* **19** 322102

[3] Yan Y X, Gambel E B Jr and Nelson K A 1985 Impulsive stimulated scattering: general importance in femtosecond laser pulse interactions with matter, and spectroscopic applications *J. Chem. Phys.* **83** 5391–9

[4] Tsen K-T, Tsen S-W D, Sankey O F and Kiang J G 2007 Selective inactivation of micro-organisms with near-infrared femtosecond laser *J. Phys.: Condens. Matter* **19** 472201

[5] Dykeman E C, Benson D, Tsen K-T and Sankey O F 2009 Simulations of impulsive laser scattering of biological protein assemblies: application to M13 bacteriophage *Phys. Rev.* E **80** 041909

[6] Dykeman E C and Sankey O F 2009 Theory of the low frequency mechanical modes and Raman spectra of the M13 bacteriophage capsid with atomic detail *J. Phys.: Condens. Matter* **21** 035116

[7] English N J and Mooney D A 2007 Denaturation of hen egg white lysozyme in electromagnetic fields: a molecular dynamics study *J. Chem. Phys.* **126** 091105

[8] Go S, Bilz H and Cardona M 1975 Bond charge, bond polarizability, and phonon spectra in semiconductors *Phys. Rev. Lett.* **34** 580–3

[9] Guha S *et al* 1996 Empirical bond polarizability model for fullerenes *Phys. Rev.* B **53** 13106–14

[10] Bermejo D, Montero S, Cardona M and Muramatsu A 1982 Transerability of the bond polarizabilities: from saturated hydrocarbons to diamond *Solid State Commun.* **42** 153–5

[11] Tsen K T, Dykeman E C, Sankey O F, Lin N-T, Tsen S-W D and Kiang J G 2006 Observation of the low frequency vibrational modes of bacteriophage M13 in water by Raman spectroscopy *Virol. J.* **3** 79

[12] Marvin D A, Welsh L C, Symmons M F, Scott W R P and Strauss S K 2006 Molecular structure of the fd (f1, M13) filamentous bacteriophage refined with respect to x-ray fibre diffraction and solid state NMR data supports specific models of phage assembly at the bacterial membrane *J. Mol. Biol.* **355** 294–309

[13] Bashford D and Case D A 2000 Generalized Born models of macromolecular solvation effects *Annu. Rev. Phys. Chem.* **51** 129

[14] Tsui V and Case D A 2001 Theory and applications of the generalized Born solvation model in macromolecular simulations *Biopolymers* **56** 275

[15] Hawkins G D, Cramer C J and Truhlar D J 1996 Parameterized models of aqueous free energies of solvation based on a pairwise descreening of solute atomic charges from a dielectric medium *J. Phys. Chem.* **100** 19824

[16] Stockley P G, Rolfsson O, Thompson G S, Basnak G, Francese S, Stonehouse N J, Homans S W and Ashcroft A E 2007 A simple, RNA-mediated allosteric switch controls the pathway to formation of a $T = 3$ viral capsid *J. Mol. Biol.* **369** 541–52

[17] Wickner W and Killick T 1977 Membrane-associated assembly of M13 phage in extracts of virus-infected *Escherichia coli* *Proc. Natl Acad. Sci. USA* **74** 505–9

[18] Cornell W D, Cieplak P, Bayly C I, Gould I R, Merz K M Jr, Ferguson D M, Spellmeyer D C, Fox T, Caldwell J W and Kollman P A 1995 A second generation force field for the simulation of proteins, nucleic acids, and organic molecules *J. Am. Chem. Soc.* **117** 5179

[19] Dykeman E C and Sankey O F 2008 Low frequency mechanical modes of viral capsids: an atomisitic approach *Phys. Rev. Lett.* **100** 028101

[20] Reddy V S, Giesing H A, Morton R T, Kumar A, Post C B, Brooks C L III and Johnson J E 1998 Energetics of quasiequivalence: computational analysis of protein–protein interactions in icosahedral viruses *Biophys. J.* **74** 546–58